IEEE Access
Multidisciplinary | Rapid Review | Open Access Journal

Received August 27, 2019, accepted September 18, 2019, date of publication October 1, 2019, date of current version October 16, 2019.

Digital Object Identifier 10.1109/ACCESS.2019.2944871

Azimuth Phase Coding by Up and Down Chirp Modulation for Range Ambiguity Suppression

WEI XU, (Member, IEEE), PINGPING HUANG, AND WEIXIAN TAN
College of Information Engineering, Inner Mongolia University of Technology, Hohhot 010050, China
Inner Mongolia Autonomous Region Key Laboratory of Radar Technology and Application, Hohhot 010050, China

Corresponding author: Wei Xu (xuwei1983@mail.imut.edu.cn)

This work was supported in part by the National Equipment Pre-Research Foundation of China under Grant JZX7Y20190253041401 and Grant JZX7Y20190253040501, in part by the Inner Mongolia Science and Technology Innovation Guidance Project under Grant KCBJ2018014, and in part by the National Natural Science Foundation of China under Grant 61631011 and Grant 61701264.

ABSTRACT High range ambiguity level will impair the spaceborne SAR image quality and hamper following SAR image applications. The range ambiguity suppression effect of the up and down chirp modulation on spaceborne SAR images is analyzed in this paper. Without taking care of ambiguity signal suppression in azimuth, the mere use of up and down chirp modulation signal would be only useful for point-liked targets and void for distributed targets. The additional azimuth phase coding introduced by the up and down chirp modulation is analyzed in this paper, and it results in Doppler spectra of part of range ambiguities shifting. Therefore, range ambiguity energy would be suppressed for both point-liked and distributed targets in spaceborne SAR with the up and down chirp modulation. The range ambiguity suppression effects of the up and down chirp modulation on both point-liked and distributed target are analyzed, and simulation results validate the presented analysis results.

INDEX TERMS Synthetic aperture radar (SAR), range ambiguity, up and down chirp modulation, azimuth phase coding.

I. INTRODUCTION

For spaceborne synthetic aperture radar (SAR), the desired radar echoes are received by the antenna after several pulse repetition intervals (PRIs) due to the long distance between the target and the radar. The preceding and succeeding pulse echoes reflected from range ambiguous areas arrive at the SAR antenna simultaneously with the desired radar echoes [1]–[4]. As a result, images of range ambiguous areas are superimposed on the SAR image of the desired area, and the quality of the SAR image is reduced. Therefore, suppressing range ambiguity energy to improve the obtained SAR image quality is very important for spaceborne SAR [5]–[7].

There are about two types of methods to suppress range ambiguity energy. One is the low level sidelobe design for the elevation antenna pattern [8]–[11] or multiple elevation beams [12], the other is frequency band pass filtering after spectra of radar echoes shifting caused by the introduced phase coding in the azimuth or range direction [13]–[17]. Alternately transmitting up and down chirp signals is considered only useful for point-liked target ambiguities but void for extended ambiguous signals [18], [19]. However, the effect of the additional azimuth phase coding is neglected during derivation of the effect of up and down chirp modulation on point and extended target signals [18]–[21]. The expression of the additional azimuth phase coding is different from the azimuth phase coding in [14], but it also results in Doppler spectra of part of range ambiguities shifting. The additional azimuth phase coding introduced by the up and down chirp modulation is derived in this paper, and the range ambiguity suppression effects on both point-liked and distributed targets are analyzed. Simulation experiments on point and distributed targets are carried out to validate the presented analysis results.

This paper is arranged as follows. Section II briefly describes the range ambiguity echo model in spaceborne SAR with the up and down chirp modulation. In Section III, the additional azimuth phase coding introduced by the up and down chirp modulation is derived. In Section IV, range ambiguity suppression effects on both point-liked and distributed targets are analyzed in detail. In Section V, simulation experiments on both point and distributed targets are carried out to validate the mentioned analysis results. Finally, the conclusion is reported in Section VI.

The associate editor coordinating the review of this manuscript and approving it for publication was Junjie Wu.

II. ECHO MODEL IN SAR WITH UP AND DOWN CHIRP MODULATION

The baseband echo signal expressions of the down and up chirp signals are written, respectively, as follows:

$$s_{\text{down}}(\tau,t)=w_a(t)\cdot\exp\left[-j\frac{4\pi R(t)}{\lambda}\right]\cdot\exp\left[-j\pi k_r\left(\tau-\tau_d(t)\right)^2\right]\cdot\text{rect}\left[\frac{\tau-\tau_d(t)}{\tau_P}\right] \tag{1}$$

$$s_{\text{up}}(\tau,t)=w_a(t)\cdot\exp\left[-j\frac{4\pi R(t)}{\lambda}\right]\cdot\exp\left[j\pi k_r(\tau-\tau_d(t))^2\right]\cdot\text{rect}\left[\frac{\tau-\tau_d(t)}{\tau_P}\right] \tag{2}$$

where τ is the fast time, t is the azimuth time, $w_a(t)$ denotes the azimuth antenna pattern, $R(t)$ is the azimuth time variant distance between the radar and the target, λ is the wave length, k_r is the chirp rate, $\tau_d(t)$ indicates the transmitted time delay, and τ_P is the transmitted pulse duration. According to the principle of stationary phase (POSP) [22], signals in (1) and (2) could be converted to the range frequency domain as follows:

$$S_{\text{down}}(f,t)=\exp\left(-j\frac{4\pi R(t)}{\lambda}\right)\cdot\frac{\exp(-j\cdot\pi/4)}{\sqrt{k_r}}\cdot\exp\left[j\pi\frac{f^2}{k_r}-j2\pi f\tau_d(t)\right]\cdot\text{rect}\left[\frac{f}{B_r}\right] \tag{3}$$

$$S_{\text{up}}(f,t)=w_a(t)\cdot\exp\left(-j\frac{4\pi R(t)}{\lambda}\right)\cdot\frac{\exp(j\cdot\pi/4)}{\sqrt{k_r}}\cdot\exp\left[-j\pi\frac{f^2}{k_r}-j2\pi f\tau_d(t)\right]\cdot\text{rect}\left[\frac{f}{B_r}\right] \tag{4}$$

where f is the range frequency, and B_r is transmitted pulse bandwidth. The matched filtering functions for the transmitted up and down chirp signals are expressed, respectively, as follows:

$$H_{\text{down}}(f)=\exp\left[-j\pi\frac{f^2}{k_r}\right]\cdot\text{rect}\left[\frac{f}{B_r}\right] \tag{5}$$

$$H_{\text{up}}(f)=\exp\left[j\pi\frac{f^2}{k_r}\right]\cdot\text{rect}\left[\frac{f}{B_r}\right] \tag{6}$$

The multiplication of the down chirp spectrum with the up chirp filtering function results in:

$$S_{\text{down}}(f,t)=\exp\left(-j\frac{4\pi R(t)}{\lambda}\right)\cdot\frac{\exp(-j\cdot\pi/4)}{\sqrt{k_r}}\cdot\exp\left[j2\pi\frac{f^2}{k_r}-j2\pi f\tau_d(t)\right]\cdot\text{rect}\left[\frac{f}{B_r}\right] \tag{7}$$

After the inverse Fourier transform (IFT) step, the signal in (7) becomes

$$s_{\text{down, defocus}}(\tau,t)=\frac{1}{\sqrt{2}}\cdot w_a(t)\cdot\exp\left[-j\frac{4\pi R(t)}{\lambda}\right]\cdot\exp\left[-j\pi\frac{k_r}{2}\left(\tau-\tau_d(t)\right)^2\right]\cdot\text{rect}\left[\frac{\tau-\tau_d(t)}{2\tau_P}\right] \tag{8}$$

With the similar processing steps, the signal with the up chirp modulation becomes

$$s_{\text{up, defocus}}(\tau,t)=\frac{1}{\sqrt{2}}\cdot w_a(t)\cdot\exp\left[-j\frac{4\pi R(t)}{\lambda}\right]\cdot\exp\left[j\pi\frac{k_r}{2}\left(\tau-\tau_d(t)\right)^2\right]\cdot\text{rect}\left[\frac{\tau-\tau_d(t)}{2\tau_P}\right] \tag{9}$$

According to (8) and (9), the following characteristics could be obtained.

- After the mismatched pulse compression step, the amplitude is lowered by $1/\sqrt{2}$ which equals to -3 dB in intensity, while the duration of the signal is doubled.
- The range linear frequency modulation is still existed, and the modulation rate is halved to $k_r/2$.

As up and down chirp pulses are alternately transmitted to suppress range ambiguities, according to (8) and (9), the defocused ambiguity echo could be written as follows:

$$s_{\text{defocus}}(\tau,n\cdot\Delta t)=\frac{1}{\sqrt{2}}\cdot w_a(n\cdot\Delta t)\cdot\exp\left[-j\frac{4\pi R(n\cdot\Delta t)}{\lambda}\right]\cdot\exp\left[j\cdot(-1)^n\cdot\varphi(\tau)\right]\cdot\text{rect}\left[\frac{\tau-\tau_d(t)}{2\tau_P}\right] \tag{10}$$

with

$$\varphi(\tau)=\pi\frac{k_r}{2}\left(\tau-\tau_d(t)\right)^2\approx\pi\frac{k_r}{2}\left(\tau-\tau_d(t_c)\right)^2 \tag{11}$$

According to (10), it can be seen that the azimuth phase modulation is existed in the defocused ambiguity echo. Furthermore, the phase $\varphi(\tau)$ is related with the fast time τ.

III. AZIMUTH PHASE MODULATION

For the simplicity, the defocused ambiguity echo in (10) is rewritten as:

$$s(n)=s_{\text{defocus}}(\tau,n\cdot\Delta t)=s_0(n)\cdot s_1(n) \tag{12}$$

with

$$s_0(n)=\frac{1}{\sqrt{2}}\cdot w_a(n\cdot\Delta t)\cdot\exp\left[-j\frac{4\pi R(n\cdot\Delta t)}{\lambda}\right] \tag{13}$$

$$s_1(n)=\exp\left[j\cdot(-1)^n\cdot\varphi\right] \tag{14}$$

Applying azimuth Discrete Flourier Transform (DFT) to (12), and we can get

$$S(k)=\text{DFT}\left(s(n)\right)=\text{DFT}\left(s_0(n)\cdot s_1(n)\right)=S_0(k)\otimes S_1(k) \tag{15}$$

where $\otimes$ is the convolution operator, while $S_0(k)$ and $S_1(k)$ are the DFT expressions of $s_0(n)$ and $s_1(n)$, respectively. $S_1(k)$ is computed as follows:

$$S_1(k) = \sum_{n=1}^{N-1} \exp\left[j \cdot (-1)^n \cdot \varphi\right] \cdot \exp\left(-j\frac{2\pi \cdot k \cdot n}{N}\right) \quad (16)$$

where N is the number of azimuth samples in SAR. Usually, N is an even number, (16) could be rewritten as follows:

$$\begin{aligned} S_1(k) = &\sum_{a=0}^{N/2-1} \left\{\exp(-j \cdot \varphi) \cdot \exp\left[-j\frac{2\pi \cdot k}{N} \cdot 2a\right]\right\} \\ &+ \sum_{a=0}^{N/2-1} \left\{\exp(j \cdot \varphi) \cdot \exp\left[-j\frac{2\pi \cdot k}{N} \cdot (2a+1)\right]\right\} \end{aligned} \quad (17)$$

If $k = 0$, $S_1(k)$ is obtained as follows:

$$S_1(k) = \frac{N}{2}\left[\exp(-j \cdot \varphi) + \exp(j \cdot \varphi)\right] = N \cdot \cos\varphi \quad (18)$$

If $k = N/2$, $S_1(k)$ is obtained as follows:

$$S_1(k) = \frac{N}{2}\left[\exp(-j \cdot \varphi) - \exp(j \cdot \varphi)\right] = j \cdot N \cdot \sin\varphi \quad (19)$$

Otherwise ($k \neq 0, k \neq N/2$), $S_1(k)$ is computed as follows:

$$\begin{aligned} S_1(k) = &\exp(-j \cdot \varphi) \cdot \frac{1 - \exp(-j2\pi \cdot k)}{1 - \exp\left(-j\frac{4\pi \cdot k}{N}\right)} \\ &+ \exp\left(j \cdot \varphi - j\frac{2\pi \cdot k}{N}\right) \cdot \frac{1 - \exp(-j2\pi \cdot k)}{1 - \exp\left(-j\frac{4\pi \cdot k}{N}\right)} \\ = &\ 0 \end{aligned} \quad (20)$$

Therefore, (17) is rewritten as

$$S_1(k) = N \cdot \cos\varphi \cdot \delta(k) + j \cdot N \cdot \sin\varphi \cdot \delta(k - N/2) \quad (21)$$

where $\delta(k)$ is the unit impulse function. Afterwards, $S(k)$ is written as

$$\begin{aligned} S(k) &= S_0(k) \otimes S_1(k) \\ &= N \cdot \cos\varphi \cdot S_0(k) + j \cdot N \cdot \sin\varphi \cdot S_0(k - N/2) \end{aligned} \quad (22)$$

As a result, after the azimuth Fourier transform step, the defocused range ambiguity in the range-Doppler domain is obtained as follows:

$$\begin{aligned} &S_{\text{defocus}}(\tau, f_a) \\ &= \frac{1}{\sqrt{2}} \cdot \text{rect}\left[\frac{\tau - \tau_d(t)}{2\tau_P}\right] \\ &\quad \cdot \left[\cos(\varphi(\tau)) \cdot W_a(f_a) + j \cdot \sin(\varphi(\tau)) \cdot W_a(f_a - \text{PRF}/2)\right] \end{aligned} \quad (23)$$

where $W_a(f_a)$ is the Doppler spectrum weighted by the azimuth antenna pattern (AAP). It can be seen that the defocused Doppler spectrum is divided into two parts as shown in Figure 1 due to the azimuth phase modulation in (14). The proportional relationship between two spectrum parts is related to the range time variant phase term $\varphi(\tau)$. Furthermore, large part of ambiguous energy could be removed out of signal processing bandwidth as shown in Figure 2(c), while PRF is selected with a relative high value.

According to (8), (9) and (23), the ratio γ between the remained and shifted Doppler spectrum parts as shown in Figure 1 in the whole pulse duration is expressed as follows:

$$\begin{aligned} \gamma(\varphi_0) &= \frac{\int_{-\tau_P}^{\tau_P} \cos^2(\pi k_r \tau^2/2 + \theta_0) d\tau}{\int_{-\tau_P}^{\tau_P} \sin^2(\pi k_r \tau^2/2 + \theta_0) d\tau} \\ &= \frac{\sum_{m=-M}^{M-1} \cos^2\left(\pi k_r (m \cdot \Delta\tau)^2/2 + \theta_0\right)}{\sum_{m=-M}^{M-1} \sin^2\left(\pi k_r (m \cdot \Delta\tau)^2/2 + \theta_0\right)} \end{aligned} \quad (24)$$

with

$$M = \tau_P \cdot f_s \quad (25)$$

where θ_0 the initial phase, f_s is the range sampling frequency, and $\Delta\tau = 1/f_s$ is the range time sampling interval. Figure 2 shows the ratio γ under different signal bandwidths, sampling frequencies and pulse durations, and it can be seen that the ratio γ almost equals to 1. The small numerical fluctuation of the ratio γ is caused by radar echo discrete sampling and could be neglected.

IV. RANGE AMBIGUITY SUPPRESSION BY UP AND DOWN CHIRP MODULATION

A. UP AND DOWN CHIRP MODULATION FOR RANGE AMBIGUITY SUPPRESS

For spaceborne SAR systems, the signal to be transmitted and scattered back to the radar should last several pulse repetition intervals (PRIs) due to the long transmitting distance between the radar and the target. Consequently, echoes scattered from the desired area and range ambiguous signals scattered from undesired areas are mixed together in the receiving window as shown in Figure 3.

Compared with the slant range history of the desired imaged area, the slant range history of range ambiguous area could be expressed as

$$r_{\text{amb},n} = r + n \cdot \frac{c}{2\text{PRF}} \quad (26)$$

where c is the velocity of the light, PRF is the pulse repetition frequency, n is the ambiguous number (negative part presents previous pulses when positive part presents latter pulses) as shown in Figure 3. Therefore, received echoes consist of signals from the desired area and range ambiguity signals from ambiguous areas are expressed as follows:

$$s(\tau, t) = s_{\text{sig}}(\tau, t) + \sum_n s_{\text{amb},n}(\tau, t) \quad (27)$$

where $s_{\text{sig}}(\tau, t)$ is radar signal from the desired area, and $s_{\text{amb},n}(\tau, t)$ represents echoes from the n-th ambiguous area. In conventional spaceborne SAR systems, the expression

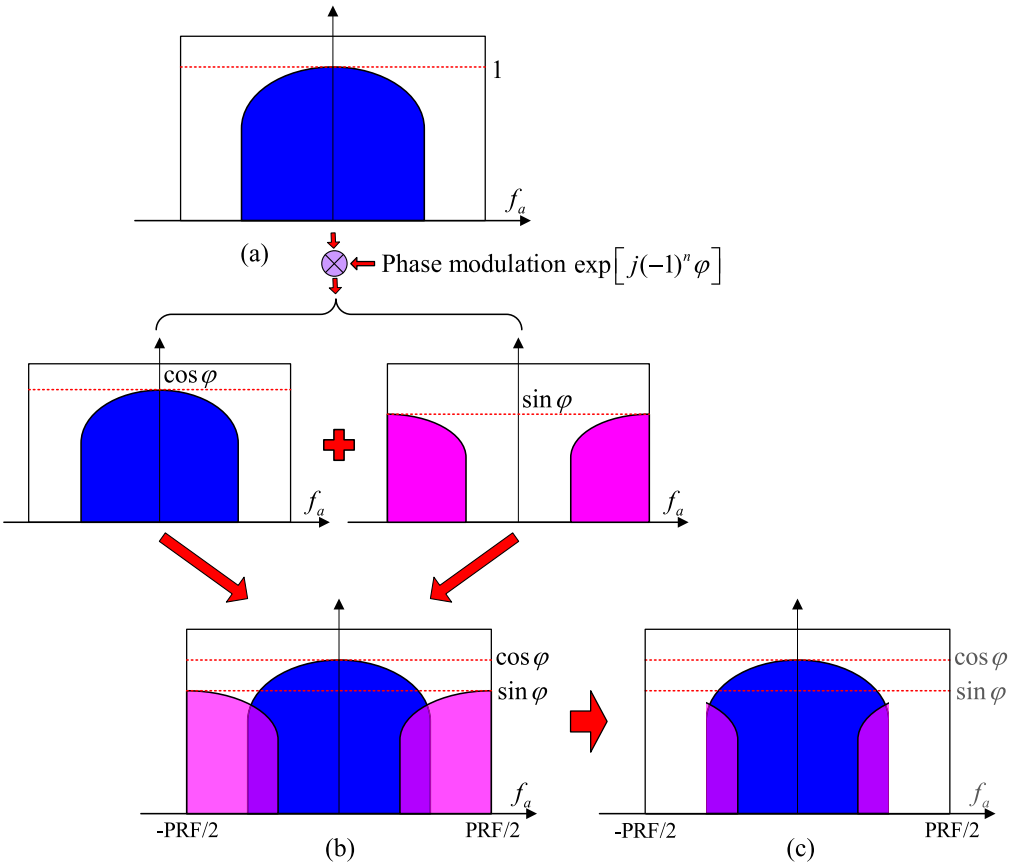

FIGURE 1. Azimuth Doppler spectra multiplied with the additional azimuth phase modulation $\exp\left[j\cdot(-1)^n\cdot\varphi\right]$. (a) Before multiplying azimuth phase modulation. (b) After multiplying azimuth phase modulation. (c) After Doppler filtering.

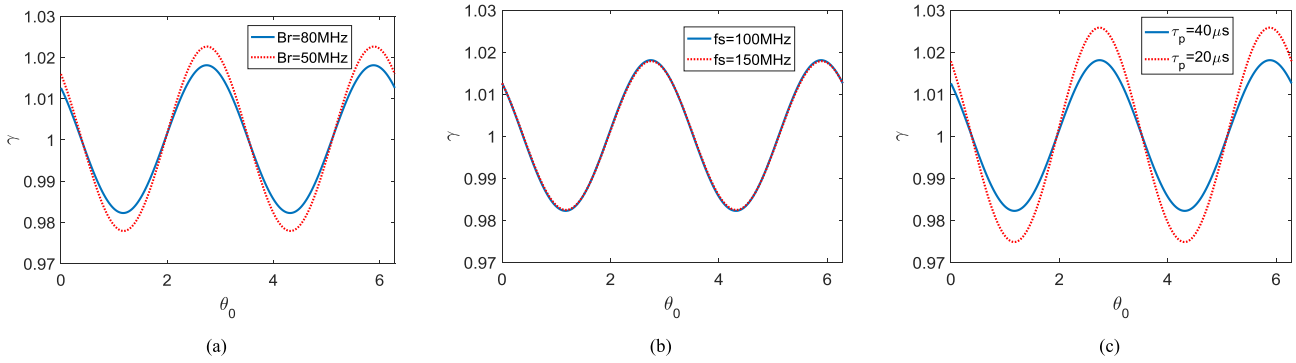

FIGURE 2. The ratio γ between the remained and shifted Doppler spectrum parts in the whole pulse duration under different cases. (a) With different pulse bandwidths. (b) With different sampling frequencies. (c) With different pulse durations.

of $s_{\text{amb},n}(\tau, t)$ is

$$s_{\text{amb}}(\tau, t; r_n) = \sigma(r_n)\cdot W_a(t; r_n)\cdot W_r\left(\frac{\tau - 2R_n(t)/c}{\tau_P}\right)\cdot\exp\left(-j\frac{4\pi R_n(t)}{\lambda}\right)\cdot\exp\left[j\pi k_r\left(\tau - \frac{n}{2\text{PRF}} - 2R_n(t)/c\right)^2\right] \tag{28}$$

where $\sigma(\cdot)$ is the backscattering intensity, $R_n(t)$ is the range history of an ambiguous point target, $W_a(\cdot)$ and $W_r(\cdot)$ indicate the azimuth and range antenna patterns, respectively.

If up and down chirp modulation signals are alternately transmitted, radar echoes from the desired area $ss_{\text{sig}}(\tau, t)$ is expressed as:

$$ss_{\text{sig}}(\tau, t; r) = \sigma(r)\cdot W_a(t; r)\cdot W_r\left(\frac{\tau - 2R(t)/c}{\tau_P}\right)$$

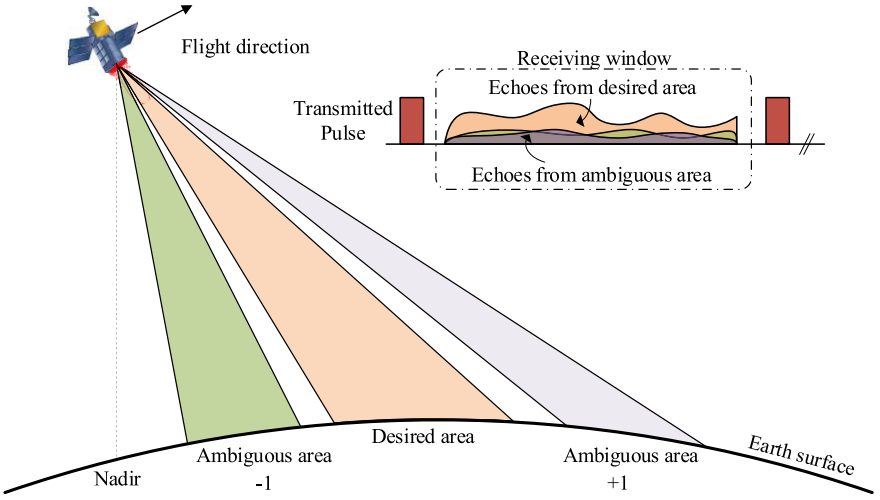

FIGURE 3. Illustration of range ambiguities received by the antenna and mixed with the desired echoes in the receiving window in spaceborne SAR.

$$\cdot \exp\left(-j\frac{4\pi R(t)}{\lambda}\right)\cdot \exp\left[j\pi k_r\left(\tau-2R(t)/c\right)^2\right]$$
$$+\sigma(r)\cdot W_a(t+\mathrm{PRI};r)\cdot W_r\left(\frac{\tau-2R(t+\mathrm{PRI})/c}{\tau_P}\right)$$
$$\cdot \exp\left(-j\frac{4\pi R(t+\mathrm{PRI})}{\lambda}\right)$$
$$\cdot \exp\left[j\pi k_r\left(\tau-2R(t+\mathrm{PRI})/c\right)^2\right] \quad (29)$$

where PRI $= 1/\mathrm{PRF}$ is the azimuth time sampling interval, and $t = 2\cdot\mathrm{PRI}$ is the azimuth in SAR with up and down chirp modulation. Consequently, the expression of $S_{\mathrm{amb,n}}(\tau, t)$ for echoes from the ambiguous area is written as:

$$ss_{\mathrm{amb}}(\tau,t;r_n)$$
$$=\sigma(r_n)\cdot W_a(t;r_n)\cdot W_r\left(\frac{\tau-2R_n(t)/c}{\tau_p}\right)$$
$$\cdot \exp\left(-j\frac{4\pi R_n(t)}{\lambda}\right)$$
$$\cdot \exp\left[(-1)^n\cdot j\pi k_r\left(\tau-2R_n(t)/c\right)^2\right]$$
$$+\sigma(r_n)\cdot W_a(t+\mathrm{PRI};r)\cdot W_r\left(\frac{\tau-2R_n(t+\mathrm{PRI})/c}{\tau_p}\right)$$
$$\cdot \exp\left(-j\frac{4\pi R_n(t+\mathrm{PRI})}{\lambda}\right)$$
$$\cdot \exp\left[(-1)^{n+1}\cdot j\pi k_r\left(\tau-2R_n(t+\mathrm{PRI})/c\right)^2\right] \quad (30)$$

Compared with (29), ambiguous signals with odd n show contrary chirp modulation rate to the desired echoes, while range ambiguities with even n show the same modulation rate as shown in Figure 4. The matched filtering with a contrary chirp modulation rate will result in the defocusing phenomenon along the range direction, and the additional azimuth phase modulation is existed in defocused range ambiguities. Therefore, only range ambiguities with odd n could be suppressed.

B. RANGE AMBIGUITY SUPPRESSION FOR POINT-LIKED TARGETS

For the comparison with (8) and (9), the result of the correct matched filtering in the frequency domain of the chirp signal is:

$$s_{\mathrm{sign},1}(\tau,t;r)=\mathrm{ext}\left(-j\frac{4\pi R(t)}{\lambda}\right)\cdot\sqrt{\tau_P B_r}\cdot\mathrm{sinc}(\pi B_r\tau) \quad (31)$$

Afterwards, the focused point target is expressed as:

$$s_{\mathrm{sig},2}(\tau,t;r)=\exp\left(-j\frac{4\pi r}{\lambda}\right)\cdot\sqrt{B_a^2/|k_a|}\cdot\mathrm{sinc}\left(\pi B_a t\right)$$
$$\cdot\sqrt{\tau_P B_r}\cdot\mathrm{sinc}\left(\pi B_r\tau\right) \quad (32)$$

where B_a is the processed Doppler bandwidth, and k_a is the azimuth chirp modulation rate. Since the desired signal and the range ambiguity are with different range cell migrations (RCMs), after the azimuth focusing step, the range ambiguity signal becomes

$$s_{\mathrm{amb}}(\tau,t)=\exp\left(-j\frac{4\pi r}{\lambda}\right)\cdot\sqrt{B_a^2/|k_a|}\cdot\frac{\rho_a}{\Delta T}$$
$$\cdot\mathrm{rect}\left[\frac{t-t_x}{\Delta T}\right]\cdot\sqrt{\frac{\tau_P B_r}{M}}\cdot\mathrm{rect}\left[\frac{\tau-\tau_r}{\Delta\tau}\right] \quad (33)$$

with

$$\Delta T=\frac{B_a}{\left|1/k_a-1/k_{a,\mathrm{amb}}\right|} \quad (34)$$

where ρ_a is the azimuth resolution, M indicates the number of range bins after RCM correction (RCMC) for the range ambiguity, while $k_{a,\mathrm{amb}}$ is the azimuth chirp modulation rate of the range ambiguity.

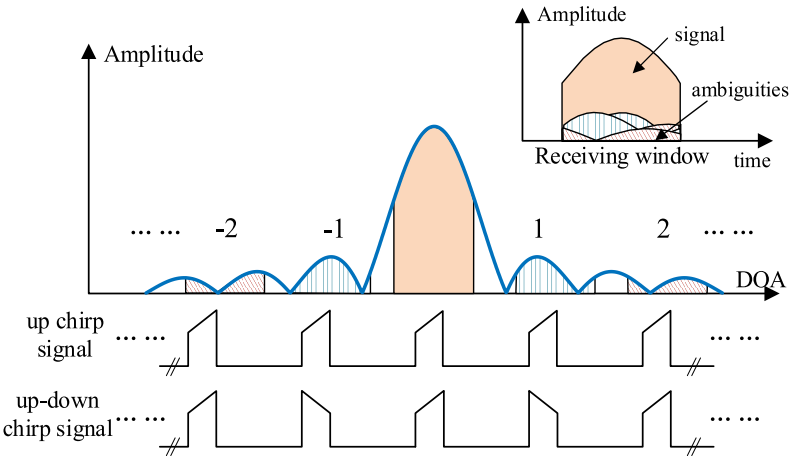

FIGURE 4. Illustration of range ambiguity suppression by up and down chirp modulation in spaceborne SAR systems.

According to (23) and Figure 1(c), after the azimuth focusing step, the odd range ambiguity signal $ss_{\text{amb,odd}}(\tau, t)$ for a point target becomes three parts as follows:

$$\begin{aligned} & ss_{\text{amb,odd}}(\tau, t) \\ &= \frac{1}{2}\exp\left(-j\frac{4\pi r}{\lambda}\right)\cdot\sqrt{B_a^2\Big/|k_a|}\cdot\frac{\rho_a}{\Delta T} \\ &\quad\cdot\text{rect}\left[\frac{t-t_x}{\Delta T}\right]\cdot\text{rect}\left[\frac{\tau-\tau_d(t_x)}{2\tau_P}\right] \\ &\quad+\frac{1}{2}\exp\left(-j\frac{4\pi r}{\lambda}\right)\cdot\sqrt{B_a^2\Big/|k_a|}\cdot\frac{\rho_a}{\Delta T_1}\cdot\chi \\ &\quad\cdot\text{rect}\left[\frac{t-t_x-\text{PRF}/|k_a|}{\Delta T_1}\right] \\ &\quad\cdot\text{rect}\left[\frac{\tau-\tau_d(t_x+\text{PRF}/|k_a|)}{2\tau_P}\right] \\ &\quad+\frac{1}{2}\exp\left(-j\frac{4\pi r}{\lambda}\right)\cdot\sqrt{B_a^2\Big/|k_a|}\cdot\frac{\rho_a}{\Delta T_1}\cdot\chi \\ &\quad\cdot\text{rect}\left[\frac{t-t_x+\text{PRF}/|k_a|}{\Delta T_1}\right] \\ &\quad\cdot\text{rect}\left[\frac{\tau-\tau_d(t_x-\text{PRF}/|k_a|)}{2\tau_P}\right] \end{aligned} \tag{35}$$

with

$$\chi = \frac{\int_{B_a/2}^{\text{PRF}/2} W_a(f_a - PRF)df_a}{\int_{-B_a/2}^{B_a/2} W_a(f_a)df_a} \tag{36}$$

$$\Delta T_1 = \frac{\text{PRF} - B_a}{2\left|1/k_a - 1/k_{a,\text{amb}}\right|} \tag{37}$$

According to the side-looking SAR imaging geometry as shown in Figure 3, compared with other ambiguous areas, echoes from ambiguous areas ($n = \pm 1$) adjacent to the imaged area are received by the elevation antenna pattern with the higher sidelobe level in most cases. Therefore, suppressing ambiguity energy of ambiguous areas adjacent to the imaged area is the most important. For a point target, the amplitude factor γ_1 is introduced to evaluate range ambiguity suppression improvement by the up and down chirp modulation and expressed as

$$\gamma_1 = \frac{\max\left\{s_{\text{amb,odd}}(\tau, t)\right\}}{\max\left\{ss_{\text{amb,odd}}(\tau, t)\right\}} = 2\sqrt{\frac{\tau_P B_r}{M}} \tag{38}$$

C. RANGE AMBIGUITY SUPPRESSION FOR EXTENDED TARGETS

To evaluate range ambiguity suppression effect on extended targets, extended targets are simply modeled being an array of point targets with same amplitude and phase [19]. The result of mismatched filtering of the echoes of a wanted extended target is directly the convolution of the extended target with the impulse response function. As a result, expressions of the first range ambiguity ($n = 1$) in a conventional SAR system and in a SAR system with the up and chirp modulation are, respectively, expressed as:

$$e_{\text{amb}} = s_{\text{amb}}(\tau, t) \otimes \sigma(\tau, t) = \iint_A s_{\text{amb}}(\tau, t)d\tau dt \tag{39}$$

$$\begin{aligned} e_{\text{amb,odd}} &= ss_{\text{amb,odd}}(\tau, t) \otimes \sigma(\tau, t) \\ &= \iint_A ss_{\text{amb,odd}}(\tau, t)d\tau dt \end{aligned} \tag{40}$$

with

$$A = d_x \cdot d_r = T_x v_g \cdot \frac{1}{2}\tau_r c \tag{41}$$

where A is the area of the range ambiguous scene, d_x and d_r denote the length of the extended target in the azimuth and range directions, respectively, v_g is the velocity of the antenna footprint, T_x and τ_r are time durations for the extended target in the azimuth and range directions, respectively.

For an extended target, the amplitude factor γ_2 is introduced to evaluate range ambiguity suppression improvement and expressed as:

$$\gamma_2 = \frac{e_{\text{amb}}}{e_{\text{amb,odd}}} = \frac{\iint_A s_{\text{amb}}(\tau, t)d\tau dt}{\iint_A ss_{\text{amb,odd}}(\tau, t)d\tau dt} \tag{42}$$

According to Figure 1, the amplitude factor γ_2 for the extended target under different cases is expressed as (43), shown at the bottom of the 10th page.

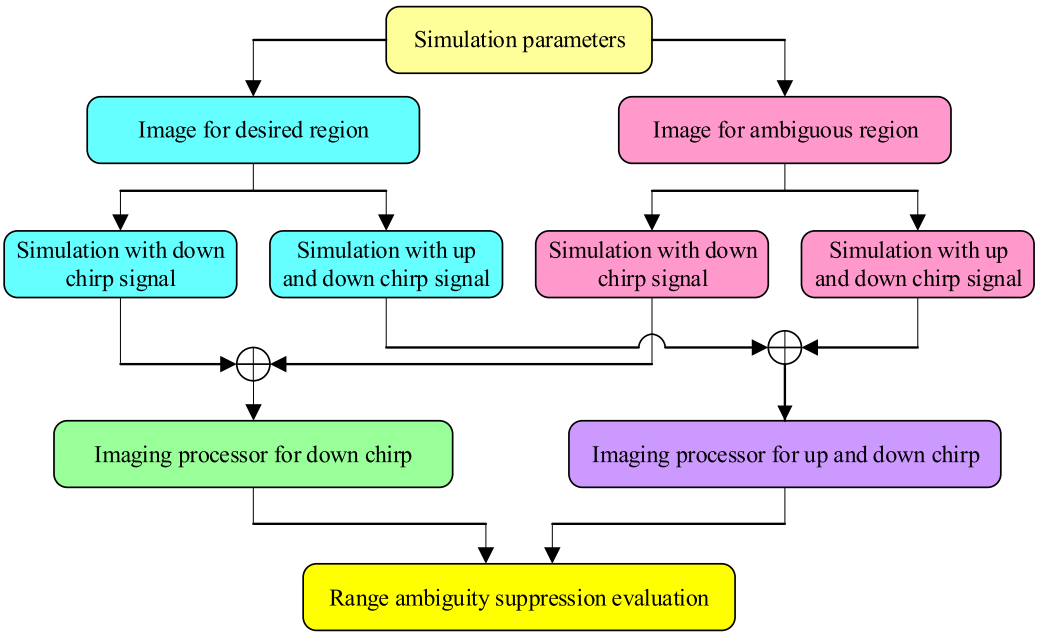

FIGURE 5. Range ambiguity suppression simulation for extended targets.

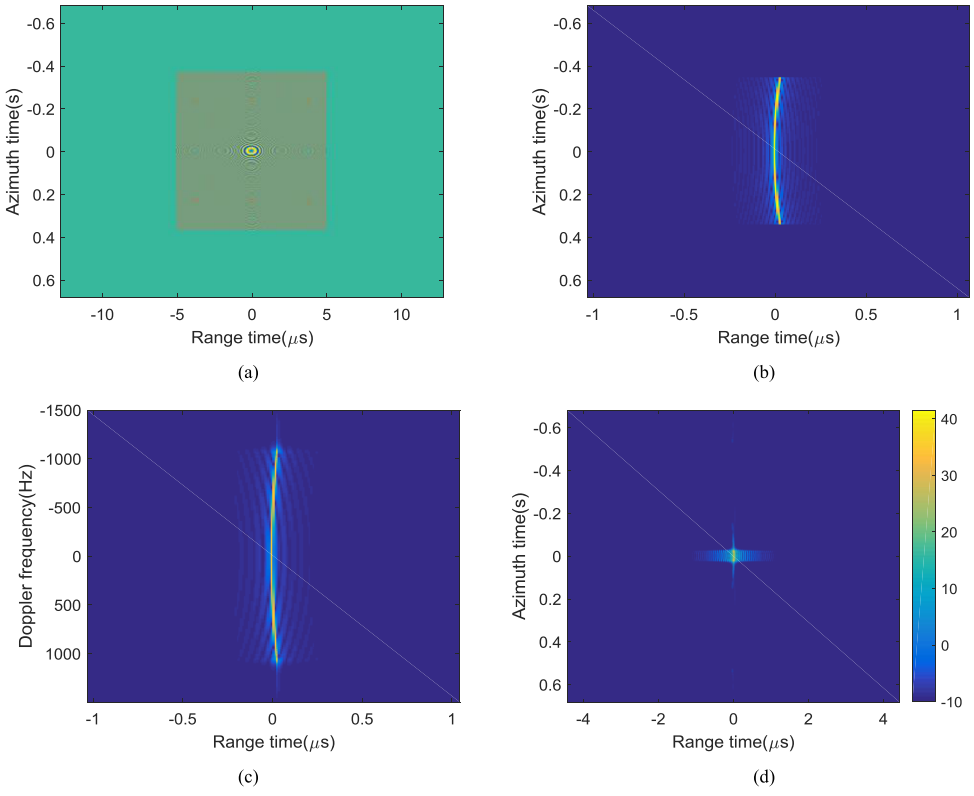

FIGURE 6. Range ambiguity imaging for a point range ambiguous target by down chirp modulation. (a) Real part of range ambiguity raw data in the two-dimensional (2D) time domain; (b) Range compression result; (c) Range compression result in the range-Doppler domain; (d) Range ambiguity after 2D focusing.

V. SIMULATION EXPERIMENTS

A. RANGE AMBIGUITY SIMULATOR

In order to evaluate the range ambiguity suppression effect of introducing the up and down chirp modulation for both point and distributed targets, a range ambiguity simulator is developed as shown in Figure 5.

The aim of the echo simulator in Figure 5 is to introduce simulated ambiguous signals into simulated "range

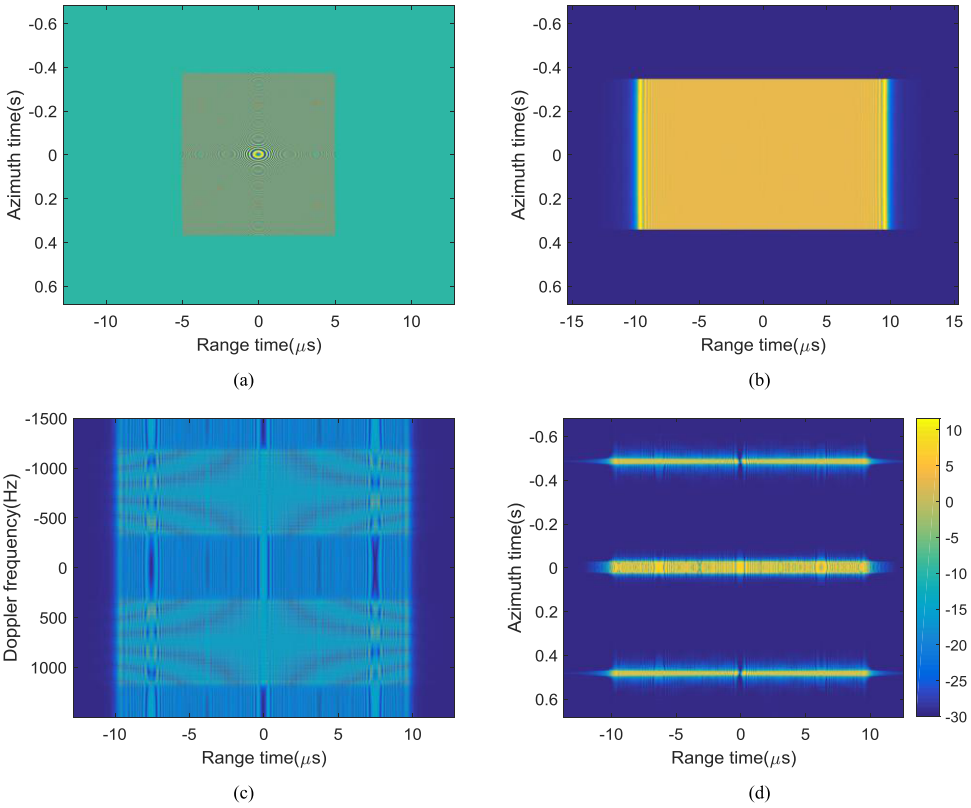

FIGURE 7. Range ambiguity imaging for a point range ambiguous target by up and down chirp modulation. (a) Real part of range ambiguity raw data in the 2D time domain; (b) Range compression result; (c) Range compression result in the range-Doppler domain; (d) Range ambiguity after 2D focusing.

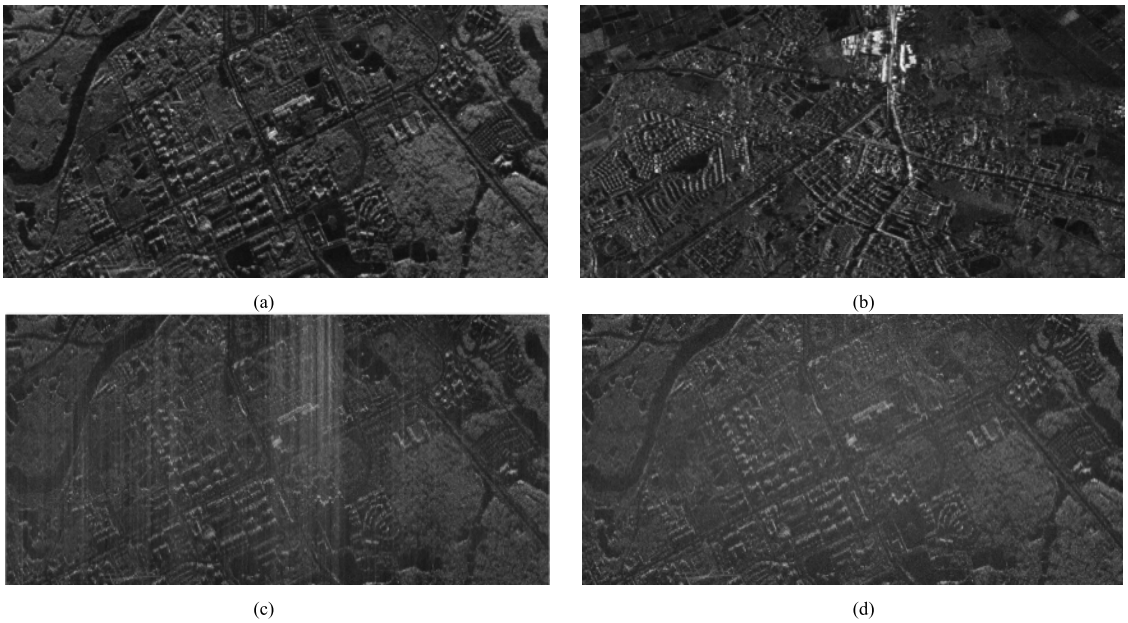

FIGURE 8. Range ambiguity suppression simulation experiment on urban scene. (a) Scene area. (b) Ambiguous area. (c) Imaging result of traditional echoes with the down chirp signal. (d) Imaging result of echoes with the up and down chirp modulation signal.

ambiguity free'' raw data to obtain ''ambiguous raw data'' [19]. As range ambiguity signals from succeeding or preceding pulses are received at the same time, parameters for range ambiguous areas including the slant range, the chirp modulation and the incidence angle could be easily obtained from parameters of the desired area. Afterwards, ''ambiguous raw data'' are handled by the imaging processor according to the chirp modulation. Finally, according to the

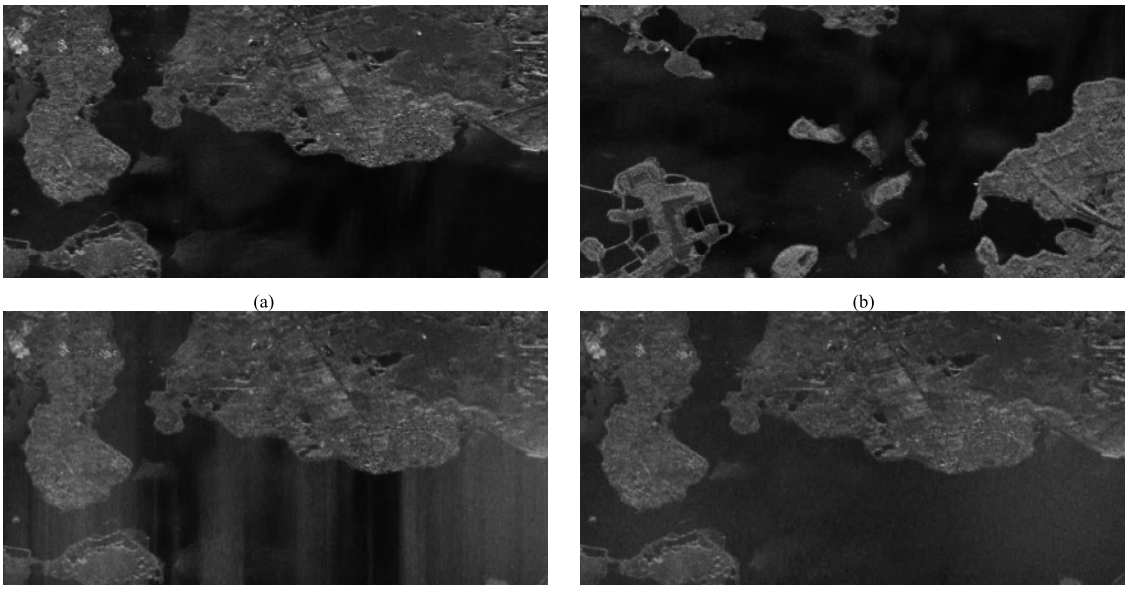

FIGURE 9. Range ambiguity suppression simulation experiment on seaside scene. (a) Scene area. (b) Ambiguous area. (c) Imaging result of traditional echoes with the down chirp signal. (d) Imaging result of echoes with the up and down chirp modulation signal.

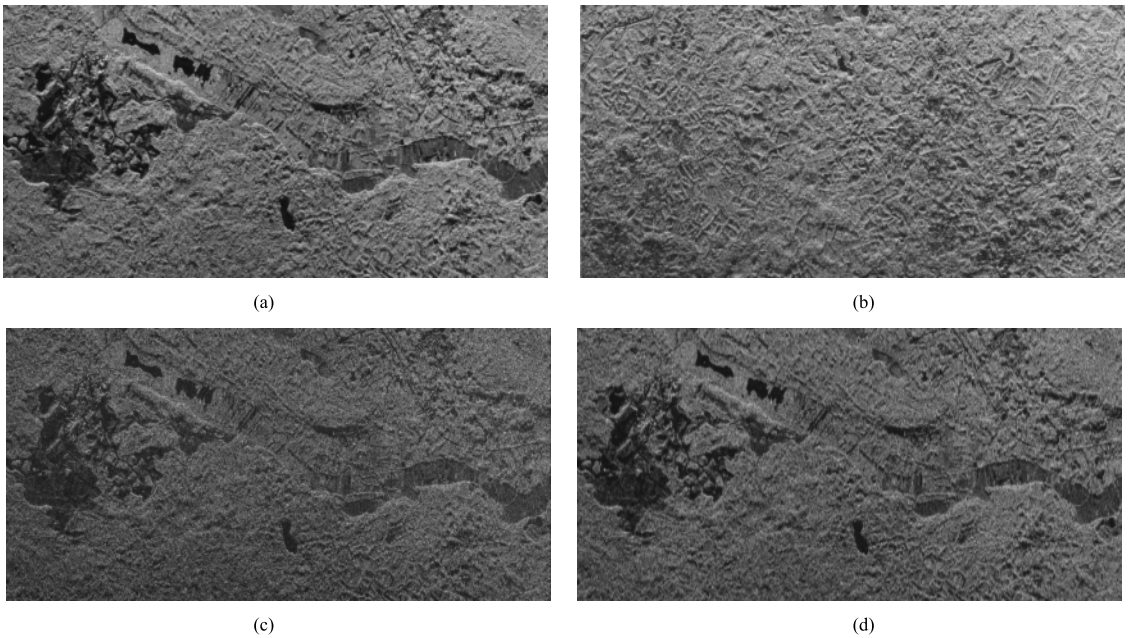

FIGURE 10. Range ambiguity suppression simulation experiment on jungle scene. (a) Scene area. (b) Ambiguous area. (c) Imaging result of traditional echoes with the down chirp signal. (d) Imaging result of echoes with the up and down chirp modulation signal.

range ambiguity to signal ratio (RASR) comparison between traditional echoes and echo with up and down chirp modulation, the RASR ambiguity suppression ability with respect to certain scene could be evaluated.

To validate the above mentioned analysis results, simulations on point and extend targets are carried out. Simulation parameters are listed in Table 1. This paper is focused on range ambiguity suppression effect of the up and down chirp modulation, and the effect of radar echoes weighted by the elevation antenna pattern is neglected for the simplicity.

B. SIMULATION EXPERIMENTS FOR POINT TARGETS

In this experiment, point ambiguity targets with the traditional down chirp modulation and with the up and down chirp

TABLE 1. System parameters.

Parameter	Value
PRF	3000 Hz
Center frequency	5.6 GHz
Pulse width	10 us
Azimuth antenna length	8 m
Signal bandwidth	80 MHz
Sampling rate	100 MHz
Orbit Height	500 km
Slant range for the scene center	700 km
Scene width	15 km
Scene length	20 km
Effective sensor velocity	7500 m/s

modulation are compared to validate the range ambiguity suppression effect by introducing the up and down chirp modulation. Figure 6 shows imaging results of a point range ambiguous target with the down chirp modulation, and the point range ambiguous target is almost focused. The little range defocusing is caused by the wrong RCMC processing, and the little azimuth defocusing is due to the mismatched azimuth modulation rate. The max value of the point range ambiguous target is 41.52dB.

Figure 7 shows imaging results of a point range ambiguous target with the up and down chirp modulation, and the point range ambiguous target is completely defocused. The contrary chirp modulation rate of the up and down chirp modulation results in the doubled pulse duration as shown in Figure 7(b), while the additional azimuth phase coding introduced by the up and down chirp modulation leads to the Doppler spectrum shifting and aliasing as shown in Figure 7(c). In the final obtained SAR image, the ambiguous target is divided into three parts as shown in Figure 7(d), and the max value of the point range ambiguous target is 11.62dB. Compared with the result in Figure 6, the RASR improvement ratio is about 30dB in this simulation experiment, and the M in (33) is about 3 due to the range resolution of the ambiguous target about three times coarser as the desired target. The total power of the impulse response in Figure 6(d) is 64.15dB, while the total power of the impulse response in Figure 7(d) is 62.60dB. The 1.55dB power reduction is caused by the Doppler spectrum band-pass filtering as shown in Figure 7(c).

C. SIMULATION EXPERIMENTS FOR EXTENDED TARGETS

The length of the designed scene is 20km, while the width is 15km. As a result, the size of the designed scene is satisfied with the second condition in (43). Evaluating the range ambiguity suppression effect for extended targets is much more complexity than point targets, since the effect obviously relies on the feature of the ambiguous area. Therefore, three typical kinds of extended scenes including urban, seaside and jungle scenes are simulated according to the simulation method in Figure 5.

Considering the complexity and otherness of real imaging scene, two parameters are assumed to describe the RASR suppression improvement of the up and down chirp modulation, which are defined as below.

- MRI (Max RASR Improvement) is denoted as the improvement of ratio of peak power between scene area and ambiguous area before and after the application of up and down chirp, which could be quantified in dB.
- ARI (Average RASR Improvement) is denoted as the improvement of ratio of average power between scene area and ambiguous area before and after the application of up and down chirp, which could be quantified in dB.

Parameters MRI and ARI introduced to evaluate the range ambiguity suppression improvement by up and down chirp modulation for different scenes as shown in Figure 8∼10 are computed and summarized in Table 2. According to measured values listed in Table 2, the up and down chip modulation shows better performance at aspect of MRI for urban scene and seaside scene, since there are some strong scatters with a small size in ambiguous areas as shown in Figure 8(b) and Figure 9(b), while the amplitude of scatters in Figure 10(b) is relatively uniform. Furthermore, the better ARI is obtained for seaside scene, since the fluctuation of image intensity is largest among these three images in Figure 8(b), Figure9 (b) and Figure 10(b). ARIs for urban and jungle scenes are almost equal to 3dB, and this value validate the above analysis result for range ambiguity suppression improvement in (43). Generally, alternately transmitting up and down chirp signals in spaceborne SAR would show better range ambiguity suppression effect for point-liked targets, while it would be also useful for extended targets according to results of Table 2.

$$\begin{cases} \gamma_2 = 2\sqrt{\tau_P B_r \dfrac{\rho_r}{d_r}}, & \text{when } T_x \le \Delta T, \quad \tau_r \le 2\tau_p \\ \gamma_2 = \sqrt{2}, & \text{when} \Delta T < T_x \le 2\text{PRF}/|k_a| - \Delta T_1, \quad \tau_r > 2\tau_p \\ \gamma_2 = \sqrt{\dfrac{1}{1-\chi}}, & \text{when } T_x > 2\text{PRF}/|k_a| + \Delta T_1, \quad \tau_r > 2\tau_p \\ \sqrt{\dfrac{1}{1-\chi}} < \gamma_2 < \sqrt{2}, & \text{otherwise} \end{cases} \tag{43}$$

TABLE 2. Parameters of range ambiguity suppression improvement for different imaged scenes.

Scene types	MRI(dB)	ARI(dB)
Urban scene	7.01	3.20
Seaside scene	7.61	5.21
Jungle scene	5.37	3.27

VI. CONCLUSION

According to the additional leaping azimuth phase coding introduced by up and down chirp modulation, alternately transmitting up and down modulated chirp signals can suppress range ambiguity energy for both small point-liked and large extended targets. For point-liked targets, the up and down chirp modulation would lead to not only the attenuation of range ambiguous energy but also the ambiguous energy reduction. For extended targets, the attenuation effect of range ambiguous energy would become less effective, but range ambiguous could be still suppressed by the band-passed Doppler filter. Furthermore, the range ambiguous energy reduction effect relies on system PRF. PRF is assumed to be a relative high value, large part of ambiguous energy could be removed out of signal processing bandwidth, which is almost the same as azimuth phase coding. If both phase coding and up and down chirp modulation methods are simultaneously adopted, only small part of ambiguous energy can be filtered, since introduced different leaping phase exists in different range gate.

REFERENCES

[1] R. O. Harger, *Synthetic Aperture Radar Systems: Theory and Design*. New York, NY, USA: Academic, 1970.
[2] J. C. Curlander and R. N. McDonough, *Synthetic Sperture Radar: Systems and Signal Processing*. Beijing, China: Publishing House of Electronics Industry, (in Chinese), 2006.
[3] J. Wu, Z. Sun, H. An, J. Qu, and J. Yang, "Azimuth signal multichannel reconstruction and channel configuration design for geosynchronous spaceborne–airborne bistatic SAR," *IEEE Trans. Geosci. Remote Sens.*, vol. 57, no. 4, pp. 1861–1872, Apr. 2019. doi: 10.1109/TGRS.2018.2869835.
[4] J. Wu, Y. Li, W. Pu, Z. Li, and J. Yang, "An effective autofocus method for fast factorized back-projection," *IEEE Trans. Geosci. Remote Sens.*, vol. 57, no. 8, pp. 6145–6154, Aug. 2019. doi: 10.1109/TGRS.2019.2904608.
[5] K. Tomiyasu, "Image processing of synthetic aperture radar range ambiguous signals," *IEEE Trans. Geosci. Remote Sens.*, vol. 32, no. 5, pp. 1114–1117, Sep. 1994. doi: 10.1109/36.312902.
[6] H. An, J. Wu, Z. Sun, and J. Yang, "A two-step nonlinear chirp scaling method for multichannel GEO spaceborne–airborne bistatic SAR spectrum reconstructing and focusing," *IEEE Trans. Geosci. Remote Sens.*, vol. 57, no. 6, pp. 3713–3728, Jun. 2019. doi: 10.1109/TGRS.2018.2886817.
[7] Q. Zhang, J. Wu, Z. Li, Y. Miao, Y. Huang, and J. Yang, "PFA for bistatic forward-looking SAR mounted on high-speed maneuvering platforms," *IEEE Trans. Geosci. Remote Sens.*, vol. 57, no. 8, pp. 6018–6036, Aug. 2019. doi: 10.1109/TGRS.2019.2903878.
[8] H. D. Griffiths and P. Mancini, "Ambiguity suppression in sars using adaptive array techniques," in *Proc. Remote Sens., Global Monit. Earth Manage.*, vol. 2, Jun. 1991, pp. 1015–1018. doi: 10.1109/IGARSS.1991.580292.
[9] G. Krieger, S. Huber, M. Villano, M. Younis, T. Rommel, P. L. Dekker, F. Q. de Almeida, and A. Moreira, "CEBRAS: Cross elevation beam range ambiguity suppression for high-resolution wide-swath and MIMO-SAR imaging," in *Proc. IEEE Int. Geosci. Remote Sens. Symp. (IGARSS)*, Jul. 2015, pp. 196–199. doi: 10.1109/IGARSS.2015.7325733.
[10] C. Lin, P. Huang, W. Wang, Y. Li, and J. Xu, "Unambiguous signal reconstruction approach for SAR imaging using frequency diverse array," *IEEE Geosci. Remote Sens. Lett.*, vol. 14, no. 9, pp. 1628–1632, Sep. 2017. doi: 10.1109/LGRS.2017.2727512.
[11] J. Xu, G. Liao, and H. C. So, "Space-time adaptive processing with vertical frequency diverse array for range-ambiguous clutter suppression," *IEEE Trans. Geosci. Remote Sens.*, vol. 54, no. 9, pp. 5352–5364, Sep. 2016. doi: 10.1109/TGRS.2016.2561308.
[12] Q. Zhao, Y. Zhang, R. Wang, Y. Deng, W. Wang, H. Zhang, and X. Wang, "Estimation and removal of strong range ambiguities in multistatic synthetic aperture radar with multiple elevation beams," *IEEE Geosci. Remote Sens. Lett.*, vol. 16, no. 3, pp. 407–411, Mar. 2019. doi: 10.1109/LGRS.2018.2875434.
[13] V. Riché, S. Méric, J. Baudais, and É. Pottier, "Investigations on OFDM signal for range ambiguity suppression in SAR configuration," *IEEE Trans. Geosci. Remote Sens.*, vol. 52, no. 7, pp. 4194–4197, Jul. 2014. doi: 10.1109/TGRS.2013.2280190.
[14] J. Dall and A. Kusk, "Azimuth phase coding for range ambiguity suppression in SAR," in *Proc. IEEE Int. Geosci. Remote Sens. Symp.*, vol. 3, Sep. 2004, pp. 1734–1737. doi: 10.1109/IGARSS.2004.1370667.
[15] J. Yang, G. Sun, Y. Wu, and M. Xing, "Range ambiguity suppression by azimuth phase coding in multichannel SAR systems," in *Proc. IET Int. Radar Conf.*, Apr. 2013, pp. 1–5. doi: 10.1049/cp.2013.0197.
[16] W. Wang, "Mitigating range ambiguities in high-PRF SAR with OFDM waveform diversity," *IEEE Geosci. Remote Sens. Lett.*, vol. 10, no. 1, pp. 101–105, Jan. 2013. doi: 10.1109/LGRS.2012.2193870.
[17] L. Guo, X. Tan, and H. Dang, "Range ambiguity suppression for multi-channel SAR system near singular points," in *Proc. IEEE Int. Geosci. Remote Sens. Symp. (IGARSS)*, Jul. 2016, pp. 2086–2089. doi: 10.1109/IGARSS.2016.7729538.
[18] G. Krieger, N. Gebert, and A. Moreira, "Multidimensional waveform encoding: A new digital beamforming technique for synthetic aperture radar remote sensing," *IEEE Trans. Geosci. Remote Sens.*, vol. 46, no. 1, pp. 31–46, Jan. 2008. doi: 10.1109/TGRS.2007.905974.
[19] J. Mittermayer and J. M. Martinez, "Analysis of range ambiguity suppression in SAR by up and down chirp modulation for point and distributed targets," in *Proc. IEEE Int. Geosci. Remote Sens. Symp.*, vol. 6, Jul. 2003, pp. 4077–4079. doi: 10.1109/IGARSS.2003.1295367.
[20] H. Mo and Z. Zeng, "Investigation of multichannel ScanSAR with up and down chirp modulation for range ambiguity suppression," in *Proc. IEEE Int. Geosci. Remote Sens. Symp. (IGARSS)*, Jul. 2016, pp. 1130–1133. doi: 10.1109/IGARSS.2016.7729286.
[21] X. Wen, X. Qiu, B. Han, C. Ding, B. Lei, and Q. Chen, "A range ambiguity suppression processing method for spaceborne SAR with up and down chirp modulation," *Sensors*, vol. 18, no. 5, p. 1454, 2018. [Online]. Available: https://www.mdpi.com/1424-8220/18/5/1454
[22] I. G. Cumming and F. H. Wong, *Digital Processing of Synthetic Aperture Radar Data: Algorithms and Implementation*. Beijing, China: Publishing House of Electronics Industry, (in Chinese), 2012.

WEI XU (M'19) was born in Jiangsu, China, in 1983. He received the M.S. degree from the Nanjing Research Institute of Electronics Technology, Nanjing, China, in 2008, and the Ph.D. degree in communication and information engineering from the Graduate University of Chinese Academy of Sciences (GUCAS), Beijing, China, in 2011.

In 2011, he joined the Department of Spaceborne Microwave Remote Sensing System, Institute of Electronics, Chinese Academy of Sciences, Beijing. Since 2018, he has been a Professor with the College of Information Engineering, Inner Mongolia University of Technology. His research interests include spaceborne /airborne synthetic aperture radar (SAR) technology for advanced modes, SAR raw signal simulation, and SAR signal processing.

PINGPING HUANG was born in Shandong, China, in 1978. He received the B.S. degree from the College of Information Engineering, Shandong University of Technology, Zibo, China, in 2003, the M.S. degree from the College of Information Engineering, Inner Mongolia University of Technology, Hohhot, China, in 2007, and the Ph.D. degree from the Graduate University of Chinese Academy of Sciences (GUCAS), Beijing, China, in 2010.

He is currently with the College of Information Engineering, Inner Mongolia University of Technology. His current major research interests include signal processing, digital beamforming, polarimetric interferometry, and spaceborne synthetic aperture radar system design.

WEIXIAN TAN was born in Hubei, China, in 1981. He received the Ph.D. degree from the University of Chinese Academy of Sciences (GUCAS), Beijing, China, in 2009.

From 2009 to 2014, he was an Associate Researcher with the Science and Technology on Microwave Imaging Laboratory, Institute of Electronics, Chinese Academy of Sciences, Beijing. Since 2015, he has been a Professor with the College of Information Engineering, Inner Mongolia University of Technology, Inner Mongolia, China. His main research interests include Airborne SAR/GB-SAR/3D SAR systems, signal processing and applications.